Crosstalk between diverse synthetic protein degradation tags in *Escherichia coli*

Nicholas C. Butzin[1,2], and William H. Mather[‡1,2,3]
[1]Department of Physics, Virginia Polytechnic Inst. and State University
[2]Center for Soft Matter and Biological Physics, Virginia Polytechnic Inst. and State University
[3]Deptartment of Biology, Virginia Polytechnic Inst. and State University

‡Corresponding author:
William Mather
Virginia Polytechnic Institute & State University
Department of Physics MC 0435
850 West Campus Drive
Blacksburg, VA 24061
USA
Email: wmather@vt.edu
Phone: 540-231-0041
Fax: 540-231-5551
Section: Research article
Key words: synthetic biology, queueing theory, protease, crosstalk, bottleneck
Running title: Crosstalk of synthetic protein degradation tags

Abstract
Recently, a synthetic circuit in *E. coli* demonstrated that two proteins engineered with LAA tags targeted to the native protease ClpXP are susceptible to crosstalk due to competition for degradation between proteins. To understand proteolytic crosstalk beyond the single protease regime, we investigated in *E. coli* a set of synthetic circuits designed to probe the dynamics of existing and novel degradation tags fused to fluorescent proteins. These circuits were tested using both microplate reader and single-cell assays. We first quantified the degradation rates of each tag in isolation. We then tested if there was crosstalk between two distinguishable fluorescent proteins engineered with identical or different degradation tags. We demonstrated that proteolytic crosstalk was indeed not limited to the LAA degradation tag, but was also apparent between other diverse tags, supporting the complexity of the *E. coli* protein degradation system.

Introduction

Proper cell behavior is maintained using a finite pool of processing resources, such as the limited pool of enzymes required for gene transcription and protein translation[1-2]. Natural biological circuits are largely thought to have evolved to buffer against the effects of limited resources, but we are beginning to understand how processing machinery can form a bottleneck that is in fact leveraged as a control or signaling mechanism[3-4]. Proteolytic (protein degrading) pathways, in particular, have been found to form functional bottlenecks in a native *E. coli* network regulating the stationary phase sigma factor S (σ^S). The protein σ^S is degraded by the ClpXP proteolysis system (ClpXP protease and its chaperones) much faster during exponential growth phase[5-6] than stationary phase[7], and the corresponding buildup of σ^S in stationary phase acts as a signal triggering the stress response system for starvation[8]. An explanation for increased stability of σ^S in stationary phase is that there are an increased number of mistranslated proteins targeted for degradation by ClpXP. Mistranslated proteins are targeted to ClpXP because they have a C-terminal SsrA tag (sometimes labeled LAA tag) due to a special transfer-messenger RNA (tmRNA) being added to mRNA to flag peptides for degradation[9-10]. These proteins compete for a limited number of proteases, especially ClpXP, which results in the formation of a "queue" of substrates for the protease that increases the apparent half-life of σ^S[8].

The complexity of natural proteolytic pathways serves as a barrier to understanding this phenomenon, and so synthetic circuits offer a valuable alternative approach[11]. It was predicted based on the theoretical modeling of a synthetic oscillator that overexpression of LAA-tagged proteins could lead to saturation of proteolytic machinery[12-13], i.e. that proteolytic machinery could be limiting. Recently, a synthetic circuit more directly demonstrated that two distinguishable fluorescent proteins engineered with ClpXP-targeting LAA-tags can lead the formation of a queue that resulted in crosstalk, such that the buildup of one protein can increase the concentration of another (Fig. 1A)[8]. Queueing theory has since been adopted to describe how competition between substrates for protease can lead to pronounced coupling and statistical correlation[8, 14-16]. The impact of proteolytic queueing competition leads to a rewiring of natural and synthetic circuits to include mutual modulation of substrate degradation rates[17]. This, in particular, applies to all but one existing bacterial synthetic oscillator, which target multiple species of protein to a common protease ClpXP[18]. One exception is the recently modified repressilator[19], where active degradation by protease was systematically removed to produce a more robust growth-dependent (dilution-dependent) oscillator, which interestingly was predicted based on a prior analysis of proteolytic competition[17].

The single protease crosstalk picture is too simplistic for native circuits, and the reliance on a single degradation pathway for bacterial synthetic oscillators presents a scalability problem that limits the complexity of circuits that can be developed. To address this issue, we investigated the crosstalk between multiple native degradation pathways in *E. coli*. This study extends a prior investigation of computational models that suggested a multi-protease proteolytic bottleneck may still contribute substantially to crosstalk in simple and complex (oscillatory) networks[20]. The influence of crosstalk in multi-protease models was evident even between substrates with substantially different affinities for a protease. Crosstalk may then be generic and complex in native networks. In particular, the different proteolytic networks of *E. coli* may exhibit strong mutual crosstalk, as only three proteases (Lon, ClpXP, and ClpAP, see Table S1) together are required to account for approximately 70%–80% of ATP-dependent degradation in bacterial cells[21-22]. These few proteases thus establish the bulk of proteolytic degradation bandwidth that is shared among a diverse set of actively degraded proteins (about 20% of newly synthesized

polypeptides are degraded[23]). This fact combined with the phenomenon of queueing coupling suggests that crosstalk between diverse cellular networks may be typical and cannot be easily relieved by the limited number of proteolytic pathways.

In this work, we used a synthetic biology approach to understand crosstalk between the proteolytic systems of *E. coli*. We designed several synthetic genes that produce fluorescent proteins with protease-targeting tags to serve as probes for and indicators of crosstalk between different protease queues. Using the same *E. coli* strain, we systematically investigated these genes in isolation and in combination. The tags that resulted in substantial degradation in isolation were further investigated for proteolytic crosstalk by co-expressing fluorescent proteins with specific tags. We observed that there is often measurable crosstalk when two fluorescent proteins engineered with identical degradation tags were targeted to the same protease, which is as expected based on the queueing analogy. We also identified a range of crosstalk strengths, ranging from undetectable to high, when proteins are selectively targeted to different protease pathways.

Results and Discussion

Multiple synthetic amino acid sequence tags target fluorescent proteins for degradation by different proteases. To study proteolytic degradation by different proteases, fluorescent proteins were engineered with different potential degradation tags on either the N-terminus or C-terminus (Table S2). Previously tested degradation tags could not be compared directly because they were characterized in different *E. coli* strains and under different conditions. To our knowledge, this is the first systematic investigation of multiple degradation tags in *E. coli*. We tested the previously determined degradation tags and several newly designed tags (Table 1A-B). Degradation tags were fused to multiple fluorescent proteins and tested for activity using a high-throughput *in vivo* microplate reader assay. All putative degradation tags tested targeted YFP for degradation (Fig. 2A and Fig. S1). HipBc20, MazE, SoxSn20, RepA15, and HipB were identified as poor degradation tags. In all upcoming experiments, only one poor degradation tag with a medium degradation rate, HipB, was tested for proteolytic crosstalk with other tags. All other tags (LAA, RepA70, MarA, and MarAn20) except SoxS were tested for proteolytic crosstalk.

The main proteases of an *E. coli* cell can be overloaded when proteins are targeted to a single protease via engineered degradation tags. Previous researchers utilized LAA tagged proteins to demonstrate that proteolytic queues form at ClpXP in the overloaded state [8]. We recreated their results using our own circuits (Fig. 3B). We then explored if other degradation tags with presumably different affinities (Fig. 1A) would result in the formation of queues and if queues could form with proteases other than ClpXP. YFP and CFP proteins were engineered with RepA70 tags for degradation by ClpAP. The fluorescence levels of RepA70-YFP were monitored as we increase the level of RepA70-CFP proteins by adding the chemical inducer IPTG. The fluorescence of RepA70-YFP increased as more RepA70-CFP was produced (Fig. 3C). This indicated that ClpAP protease can be overloaded, and a proteolytic-queue forms, similar to what was observed with the LAA tagged proteins targeted to ClpXP[8]. We also tested two other tags, MarA and MarA20 (20 amino acids from the N-terminal of MarA), which target proteins to be degraded by the Lon protease. The Lon protease was weakly overloaded by MarA tagged proteins, but was overloaded more by MarAn20 tagged proteins (Fig. 3C-D). This made us wonder if Lon could be overloaded when both MarA and MarAn20 were co-produced. Indeed, this was the case (Fig. 3E).

The main proteases of *E. coli* can exhibit different levels of crosstalk depending on the degradation tags used. We have demonstrated that ClpXP, ClpAP, and Lon can be overloaded using two proteins engineered with identical degradation tags targeted for a specific protease. We have hypothesized that crosstalk between proteases may occur through shared information (Fig. 1B). To test this hypothesis in a synthetic system, we monitored the level of a fluorescent protein (YFP) targeted to one protease while producing another protein (CFP) targeted to a different protease. There was strong crosstalk when proteins with the LAA degradation tag (target to ClpXP) were co-produced with proteins with all other tags (RepA70, MarA, MarAn20, and HipB; Fig. 4A-D). Although ClpXP is the primary protease that degrades LAA-tagged proteins[9, 24], several other proteases recognize this tag (Table S1). Perhaps due to the importance of removal of potentially harmful waste proteins, cells evolved to have "backup" (a cellular redundancy) proteolytic pathways to remove peptides even if ClpXP is overloaded. Although LAA-tagged proteins are often utilized in synthetic biology circuits[18], our results suggest it is not an ideal candidate for orthogonal circuits that depend on a proteolytic pathway such as most oscillators. We have tested several other degradation tags that can be potentially used in future synthetic circuits. There was measurable crosstalk when proteins with RepA70 and MarA degradation tags were co-produced (Fig. 4E), but no detectable crosstalk when MarAn20 and RepA70 tagged proteins were co-produced (Fig. 4F). This suggests that MarAn20 and RepA70 may be useful for future synthetic circuits. All proteins with the degradation tags tested thus far were rapidly degraded. We tested a medium-degradation tag, HipB, and, interestingly, we observed no apparent crosstalk between proteins with HipB-tags and all other tagged tested tags (Fig. S2), except for the LAA tag (Fig. 4D).

Single-cell data from microscopy slides support the high-throughput microplate data. The high-throughput microplate batch data allowed us to get an overall picture of the queueing phenomena with a gradient of inducer concentrations, but it is an average measurement of 1000's of cells. Analysis of single-cell images is an independent technique that is more sensitive than batch data. Single-cell analysis is less subjected to the averaging effects characteristic of batch (population-scale methods) and offers a level of discrete detection that is unobtainable with traditional microbiological techniques[25]. Single-cell data and microplate batch data had similar results when proteins were targeted to the same proteolytic pathways, although crosstalk is more apparent with the single-cell data, especially for the RepA70 tag (Fig. 5A). The single-cell data and microplate batch data also had similar results when proteins were targeted to different pathways (Fig. 5B and Fig. S3). The only minor difference detected by these methods was when proteins with RepA70 and MarA were co-produced. The batch data showed weak crosstalk (crosstalk was only detected at the highest Dox concentration; Fig. 4E), while the single-cell data showed no apparent crosstalk (Fig. 5B).

Conclusion

Using synthetic circuits, we demonstrated that crosstalk could arise between several different proteolytic pathways. We first characterized a collection of amino acid sequences (tags) that target proteins towards active degradation. Proteins fused to these tags were expressed in a common strain using identical promoters and identical plasmid origins, which allowed us to compare fairly the effectiveness of these tags as degradation signals. This initial characterization of molecular parts is itself of value to synthetic biology. We then co-expressed YFP and CFP with generally different tags to determine crosstalk between pathways. The LAA tag was particularly prone to exhibiting crosstalk with itself and other tags. Other tag combinations demonstrated a range of crosstalk, though not as strong as we measured with LAA. Since many current synthetic systems rely on proteins engineered with LAA tags (targeted to ClpXP)[12, 16, 18, 26-35], our results strongly suggest that proteolytic crosstalk may be a

major hurdle to scalability, indicating that new protease tags are required. Our select pairs of degradation tags with minimal to moderate crosstalk may have future applications in this direction, e.g. in the development of the first synthetic orthogonal to semi-orthogonal oscillators. Of course, tags with strong crosstalk may still be of value, as they could be used for more coordinated modules.

Our findings have implications for both the study of natural systems and the design of complex synthetic systems. In natural systems, cells may use transcriptional regulation and proteolytic coupling as a form of regulation based on the desired response. Transcriptional regulation allows for either a coupled or an uncoupled response. Proteolytic coupling has advantages over a transcriptional response; it may be a quicker mechanism that requires less energy. A transcriptional response to an overloaded protease requires transcription of RNA, production of protein, protein folding, and removal of excess protease after the overabundant substrates are removed. In contrast, proteolytic queueing utilizes other proteases already present in the cell, thus a subsequent response is quick and requires no additional energy to be effective nor to remove the protease later. This means cells can respond to misfolded proteins and the environmental conditions that cause an increase in faulty translation without significantly slowing growth. *E. coli* utilizes proteolytic queues for σ^S regulation[8]. Our recent stochastic models suggest that other natural systems such as toxin-antitoxin mechanism used to modulate bacterial persistence may also be augmented by proteolytic queues[20].

Methods

Reagents. All of the reagents were reagent grade and purchased from Sigma-Aldrich, Fisher Scientific, or Thomas Scientific unless otherwise stated.

Strains and Plasmids. All strains were derived from *E. coli* DH5alphaZ1 (purchased from Dr. Rolf Lutz). All of the plasmid DNA sequences (in GenBank format) are provided in the supporting Information (**Zip file 1**). CFP and YFP gene derivatives were cloned downstream of the P_{LtetO} of p31Cm (chloramphenicol 10 μg/ml)[16] or downstream of the $P_{lac/ara}$ of p24Km (kanamycin 25 μg/ml). The plasmid p24Km was constructed by PCR amplification and cloning of a T1 terminator into KpnI-ClaI restriction sites of pZE24MCS (purchased from Dr. Rolf Lutz). The CFP and YFP gene derivatives (**Table 1; Table S2**) were purchased from ThermoFisher or GenScript. The cultures were grown in Lysogeny broth (LB).

Absorbance and fluorescence measurements with a microplate reader. Cells were passed (1:250 dilution) from an overnight culture or a culture stored at 4° C for less than two weeks into LB and antibiotics. Cells were grown at 37° C at a shaking rate of 250 rpm for 2-3 h, and then 100 μl cell culture was added to individual wells of a 96-Well Optical-Bottom Plates with Polymer Base (ThermoFisher) already containing 100 μl of regents (LB, antibiotics, and inducers). A Cytation 3 microplate reader (BioTek) was used to grow and monitor cells. Cell growth was measured at OD_{600} (Optical density at 600 nm). The excitation and emission (Ex/Em) used for YFP and CFP were 510/540 and 447/477 nm, respectively. The wavelengths for Ex/Em were empirically determined to minimize crosstalk between different fluorescent proteins. The background of the media (median absorbance and mean YFP fluorescence) was subtracted from the raw reads. The fluorescence values were compared at $OD_{600\ nm}$ ~0.4 (mid-log growth phase) and then the fluorescent values were normalized by dividing by the OD. Four biological replicas were used to calculate the mean fluorescence and standard deviation.
Bleed-through from one fluorescent channel into another was tested by two different methods. First, the potential bleed-through from the YFP channel into the CFP channel was tested by

producing untagged YFP (the brightest YFP derivative) at different doxycycline (Dox) concentrations (inducing YFP) and monitoring CFP production. A similar test was done with only the untagged CFP protein (induced by isopropyl β-D-1-thiogalactopyranoside (IPTG) and arabinose). No apparent bleed-through was detected in the CFP channel when YFP was produced (Fig. S4A) and no apparent bleed-through was detected in the YFP channel when CFP was produced (Fig. S4B). Second, bleed-through was tested with *E. coli* strains carrying both untagged fluorescent proteins CFP and YFP. No apparent bleed-through was detected in the CFP channel when YFP was produced (Fig. S4C), and no apparent bleed-through was detected in the YFP channel when CFP was produced (Fig. S4D) despite carrying genes for both fluorescent proteins.

Single-cell snapshots. Cells were harvested from microplate reader wells at mid-log growth phase (near $OD_{600\ nm}$ 0.4) and single-cell snapshots were taken on a Nikon Ti microscope with CFP and YFP fluorescence cubes at 1000× magnification (a 100× objective coupled to additional 10× magnification). Phase-contrast images and fluorescence images were taken. All fluorescence images were taken with the same exposure (75 ms) and light intensity (6% solo-intensity) based on bleed-through tests. We empirically determined these settings had no apparent bleed-through (Fig. S5).

Analysis of Mean Fluorescence. To analyze single-cell snapshots, we used a custom pipeline for single-cell segmentation based on machine learning techniques. This process leveraged a FastRandomForest classifier trained and then applied using the Trainable Weka Segmentation tool in Fiji[36]. The classifier used phase contrast images (with pixel values normalized to a common mean and standard deviation) to identify individual cells that were in focus (Fig. S6), and the resulting segmented regions were saved as a separate collection of segmented images. Segmented images were then processed by custom Python 2.7 scripts using the SciPy and OpenCV packages. These scripts both measured single cell fluorescence in corresponding fluorescence images and also computed single cell statistics.

Model Fitting to Single Tag Microplate Data. Fluorescence data for the single tag constructs in microplate experiments were fit to a simple enzymatic degradation model in order to describe the data points by a mathematical function. We checked whether the measured YFP-tag fluorescence Y_T (for a range of tags T) for a given concentration $[DOX]$ could be described by the steady-state of the ODE:

$$\frac{dY_T}{dt} = \alpha \cdot \left(\frac{[DOX]^n}{C_0^n + [DOX]^n}\right) - Y_T - \frac{\mu_T Y_T}{K_T + Y_T} \qquad (1)$$

i.e., with Y_T the solution to the equation

$$0 = \alpha \cdot \left(\frac{[DOX]^n}{C_0^n + [DOX]^n}\right) - Y_T - \frac{\mu_T Y_T}{K_T + Y_T} \qquad (2)$$

In this model, we have rescaled time such that the dilution rate is 1.0, and we allow the apparent enzymatic velocity μ_T and molar constant K_T to, in principle, have independent values for each tag. The parameters α and C_0 characterize the production rate of protein for a given level of $[DOX]$. We assume that untagged YFP proteins are degraded with zero enzymatic velocity, i.e. $\mu_{Untagged} = 0$. All data points, excepting data for YFP-RepA15, were jointly fit to this model using the scipy.optimize.minimize function from the SciPy library. Parameter values for one of our best fits are reported in SI Table S3, and the fit is displayed graphically in SI Fig. S1. It is worth noting that if a fitted value for K_T is large relative to typical values of Y_T, then the relevant

degradation parameter is the first-order degradation rate constant, μ_T/K_T, and only this ratio is likely very meaningful regarding model fit.

Acknowledgements
Funding for this research was provided by the 454 National Science Foundation under Grant No. MCB-1330180.

Figures and Tables

Fig. 1. (A) Previous researchers have demonstrated that a queue can form through competition for degradation using fluorescent proteins (CFP and YFP) targeted (through the LAA tag) to the same protease ClpXP[8]. **(B)** We tested if two tags that are specific targets to two different proteases (P1, P2) could form queues.

Fig. 2. Batch single degradation tag results. YFP derivatives were expressed from the P_{LtetO} promoter using the chemical inducer doxycycline (Dox) at 200 ng/ml. A high-throughput *in vivo* microplate reader assay was used to determine the fluorescent level of proteins with and without degradation tags. The percentage degradation was calculated in this manner: 100% X (1 - $YFP_{tag}/YFP_{untagged}$) and standard deviations were calculated using a Taylor expansion[7]. This assumed that untagged YFP is at maximum production and this avoids dividing by a small number. The percentage degradation was calculated for proteins induced at different concentrations of Dox (using data from Fig. S1). Four biological replicas were used to calculate the mean fluorescence and standard deviation from *in vivo* microplate reader batch data.

Fig. 3. Degradation queues form when the proteins are engineered with degradation tags targeted to the same proteolytic pathway. (A) LAA-tagged proteins targeted to ClpXP had the strongest apparent crosstalk, while (**B**) RepA70-tagged proteins target to ClpAP had weak crosstalk compared to what was determined for LAA-tagged proteins. (**C**) MarA tagged proteins targeted to Lon had weak crosstalk, but (**D**) MarAn20-tagged (20 amino acids from the N-terminal of MarA) proteins also targeted to Lon had greater crosstalk. (**E**) Production of CFP-MarAn20 resulted in an increased level of YFP-MarA indicating crosstalk between these two tags targeted to the Lon protease. YFP derivatives were expressed from the P_{LtetO} promoter using the inducer Dox, while CFP derivatives were expressed from $P_{lac/ara}$ promoter using inducer 0.5 mM IPTG (all experiments contained 1% arabinose). Each tag comparison is indicated by tag/tag with CFP being the first tagged and YFP being the second tagged protein. Four biological replicas were used to calculate the mean fluorescence and standard deviation from *in vivo* microplate reader batch data. FU: arbitrary fluorescence unit.

Fig. 4. The main proteases of an *E. coli* cell can have different levels of proteolytic crosstalk depending on the degradation tags utilized. Strong crosstalk was detected when proteins with the LAA-tag (targeted to ClpXP) was co-produced with (**A**) RepA70, (**B**) MarA, (**C**) MarAn20, and (**D**) HipB tagged proteins. Proteins engineered with (**E**) RepA70 and MarA tags, and (**F**) MarAn20 and RepA70 tags had measurable crosstalk and no detectable crosstalk, respectively. YFP derivatives were expressed from the P_{LtetO} promoter using the inducer Dox, while CFP derivatives were expressed from $P_{lac/ara}$ promoter using inducer 0.5 mM IPTG (all experiments contained 1% arabinose). Each tag comparison is indicated by tag/tag with CFP being the first tagged and YFP being the second tagged protein. Four biological replicas were used to calculate the mean fluorescence and standard deviation from *in vivo* microplate reader batch data. FU: arbitrary fluorescence unit.

Fig. 5. Analysis of crosstalk using both single-cell and batch data. Single-cell data and microplate batch data had similar results with (**A**) proteins engineered with degradation tags targeted to the same protease, and (**B**) proteins engineered with degradation tags targeted to the different proteases. Crosstalk with HipB-tagged proteins was also determined using these methods (Fig. S3). Single-cell data was acquired by imaging cells at 1000X magnification with and without IPTG (inducing CFP derivatives) using a fluorescent confocal microscope. Cells were identified and fluorescence levels were calculated using Fiji, machine learning, and in-house scripts (see Methods). The percentage crosstalk was calculated in this manner:

100%· (1 – $YFP_{No\ IPTG}/YFP_{0.5\ mM\ IPTG}$) with the standard deviation and SEM calculated using a Taylor expansion [7]. Use of this ratio avoids dividing by a small number and reduces the impact of statistical error. Each tag comparison is indicated by tag/tag with CFP being the first tagged protein and YFP being the second tagged protein. For each single-cell fluorescent data set, the mean and SEM were calculated from 441-1133 individual cells. For *in vivo* microplate reader batch data, four biological replicas were used to calculate the mean fluorescence and standard deviation. YFP derivatives were expressed from the P_{LtetO} promoter using Dox 200 ng/ml, while CFP derivatives were expressed from $P_{lac/ara}$ promoter using 0.5 mM IPTG (all experiments contained 1% arabinose). *These values are less than (but near) zero.

Table 1. (A) Degradation tags and (B) source (*E. coli* K12 MG1655).

(A)

Tag	Tag detail	Major protease target	Minor protease target
LAA	Serves as the target for cellular ATP-dependent proteases[9, 24].	ClpXP[9, 24]	ClpAP, Lon, FtsH, Tsp (Prc)[9]
RepA70	A high-affinity substrate of ClpAP that is degraded poorly by ClpXP[37].The N-terminus of RepA is required for recognition by ClpAP[38].	ClpAP[39]	ClpXP[39]
RepA15	The N-terminus of RepA is required for recognition by ClpAP[38, 40]. Adding the adapter KLAAALE results in increased degradation[41].	ClpAP[39]	ClpXP[39]
SoxS	The amino-terminus of SoxS appears to be important for proteolytic degradation of SoxS[42].	Lon[42]	FtsH[42]
SoxSn20	This study.	Lon	
MarA	The amino-terminus of MarA appears to be the target of Lon[42].	Lon[42]	
MarAn20	This study.	Lon	
MazE	ClpAP degrades MazE[43]. Lon also degrades MazE under amino acid starvation[44].	ClpAP[43]	Lon[44]
HipB	Fast degradation of HipB is dependent on the presence of Lon[45]. When HipB is bound to HipA the DNA-bound form of HipB forms a compact dimer, but the last 16 amino acid residues are disordered. This disordered part of HipB functions has been suggested as a recognition site for Lon[46].	Lon[44-46]	
HipBc20	This study.	Lon	

(B)

Protein	Function	Locus tag
SoxS	A superoxide response regulon transcriptional activator. SoxS induces sox regulon when superoxide levels increase[47].	b4062
MarA	A multiple antibiotic resistance transcriptional regulator[48].	b1531
MazE	The antitoxin that inhibits the toxin MazE[49].	b2783
HipB	The antitoxin that inhibits the toxin HipA[50].	b1508
RepA	A plasmid P1 initiator protein[51].	Plasmid origin

Supporting Information Tables and Captions

Table S1. Key cytoplasmic proteases and chaperones.

	Function	Log growth phase	Stationary growth phase
Lon	Contains an ATPase domain to unfold substrates and translocate them to the proteolytic domain[52].	Undetermined	Undetermined
ClpP	The proteolytic domain that forms a complex with ClpA or ClpX[52].	100 molecules[53]	250–300 molecules[53]
ClpA	The ATPase domain that acts as chaperones, which can unfold substrates in the absence of ClpP[52].	40–50 hexamers[53]	150 hexamers[53]
ClpX	The ATPase domain that acts as chaperones, which can unfold substrates in the absence of ClpP[52].	75–100 hexamers[53]	90-120 hexamers[53]
SspB	Enhances degradation of SsrA-tagged proteins by ClpXP[54], but substantially decrease degradation by ClpAP[55].	140–160 dimers[53]	170-190 dimers[53]
ClpS	An adaptor protein to the ClpA[56] and forms a complex with ClpAP, ClpAPS complex[56]. ClpS inhibited the rate of ClpAP degradation of the C-terminus SsrA tagged protein, while the rate of ClpXP degradation is unaffected by ClpS[56].	250–300 molecules[53]	250–300 molecules[53]

Table S2. Plasmids and strains. (**A**) The parent plasmids were either p31Cm or p24Km plasmid. (**B**) *E. coli* strains were derived from DH5alphaZ1. Arabinose + IPTG, and Dox induce genes under the control of the $P_{lac/ara}$ and P_{LtetO} promoters, respectively. aa: amino acids.

(A) Plasmid	**Promoter**	**Tag**	**Tag terminal**	**Tag detail**
p31Cm	P_{LtetO}	None	Untagged	
p31CmNB02	P_{LtetO}	YFP	Untagged	
p31CmNB95	P_{LtetO}	YFP-LAA	C	11 aa LAA tag
p31CmNB44	P_{LtetO}	YFP-RepA15	C	15 aa from the N-terminal of RepA15 with KLAAALE linker
p31CmNB04	P_{LtetO}	RepA70-YFP	N	70 aa from the N-terminal of RepA
p31CmNB88	P_{LtetO}	YFP-SoxS	C	SoxS with TS linker
p31CmNB89	P_{LtetO}	YFP-SoxSn20	C	20 aa from the N-terminal of SoxS with TS linker
p31CmNB90	P_{LtetO}	YFP-MarA	C	MarA with TS linker
p31CmNB91	P_{LtetO}	YFP-MarAn20	C	20 aa from the N-terminal of MarA with TS linker
p31CmNB92	P_{LtetO}	YFP-MazE	C	MazE with TS linker
p31CmNB93	P_{LtetO}	YFP-HipB	C	HipB with TS linker
p31CmNB94	P_{LtetO}	YFP-HipBc20	C	20 aa from the C-terminal of HipB with TS linker
p24Km	$P_{lac/ara}$	None	Untagged	
p24KmNB83	$P_{lac/ara}$	CFP	Untagged	
p24KmNB82	$P_{lac/ara}$	CFP-LAA	C	11 aa LAA tag
p24KmNB07	$P_{lac/ara}$	RepA70-CFP	N	70 aa from the N-terminal of RepA
p24KmNB75	$P_{lac/ara}$	CFP-SoxS	C	SoxS with TS linker
p24KmNB76	$P_{lac/ara}$	CFP-SoxSn20	C	20 aa from the N-terminal of SoxS with TS linker
p24KmNB77	$P_{lac/ara}$	CFP-MarA	C	MarA with TS linker
p24KmNB78	$P_{lac/ara}$	CFP-MarAn20	C	20 aa from the N-terminal of MarA with TS linker
p24KmNB79	$P_{lac/ara}$	CFP-MazE	C	MazE with TS linker
p24KmNB80	$P_{lac/ara}$	CFP-HipB	C	HipB with TS linker
p24KmNB81	$P_{lac/ara}$	CFP-HipBc20	C	20 aa from the C-terminal of HipB with TS linker

(B) Strain	Plasmids	$P_{lac/ara}$ promoter	P_{LtetO} promoter
DZ66	p24KmNB82, p31CmNB95	CFP-LAA	YFP-LAA
DZ67	p24KmNB07, p31CmNB95	RepA70-CFP	YFP-LAA
DZ68	p24KmNB77, p31CmNB95	CFP-MarA	YFP-LAA
DZ69	p24KmNB78, p31CmNB95	CFP-MarAn20	YFP-LAA
DZ70	p24KmNB80,p31CmNB95	CFP-HipB	YFP-LAA
DZ72	p24KmNB82, p31CmNB04	CFP-LAA	RepA70-YFP
DZ33	p24KmNB07, p31CmNB04	RepA70-CFP	RepA70-YFP
DZ73	p24KmNB77, p31CmNB04	CFP-MarA	RepA70-YFP
DZ74	p24KmNB78, p31CmNB04	CFP-MarAn20	RepA70-YFP
DZ75	p24KmNB80, p31CmNB04	CFP-hipB	RepA70-YFP
DZ77	p24KmNB82, p31CmNB90	CFP-LAA	YFP-MarA
DZ78	p24KmNB07, p31CmNB90	RepA70-CFP	YFP-MarA
DZ79	p24KmNB77, p31CmNB90	CFP-MarA	YFP-MarA
DZ80	p24KmNB78, p31CmNB90	CFP-MarAn20	YFP-MarA
DZ81	p24KmNB80, p31CmNB90	CFP-HipB	YFP-MarA
DZ83	p24KmNB82, p31CmNB91	CFP-LAA	YFP-MarAn20
DZ84	p24KmNB07, p31CmNB91	RepA70-CFP	YFP-MarAn20
DZ85	p24KmNB77, p31CmNB91	CFP-MarA	YFP-MarAn20
DZ86	p24KmNB78, p31CmNB91	CFP-MarAn20	YFP-MarAn20
DZ87	p24KmNB80, p31CmNB91	CFP-HipB	YFP-MarAn20
DZ89	p24KmNB82, p31CmNB93	CFP-LAA	YFP-hipB
DZ90	p24KmNB07, p31CmNB93	RepA70-CFP	YFP-hipB
DZ91	p24KmNB77, p31CmNB93	CFP-MarA	YFP-hipB
DZ92	p24KmNB78, p31CmNB93	CFP-MarAn20	YFP-hipB
DZ93	p24KmNB80, p31CmNB93	CFP-HipB	YFP-hipB

Table S3. Extracted parameters for single tag fluorescence data. A simple model based on enzymatic degradation was fit to fluorescence data to produce smooth curves that fit through the data. The parameters producing the best fit for this model are contained in this table. These parameters are used in SI Fig S1. Interestingly, the K values for the most rapidly degrading species (LAA, RepA70, and MarA) are the smallest estimated values for K, suggesting higher affinity enzymatic degradation for these species. All parameters are dimensionless or arbitrary units, excepting for the constant C_0.

Parameter	Value	Parameter	Value
n	3.40	K_{MarA}	8022
C_0 (ng/ml)	132.93	μ_{MarA}	86793
α	10597	$K_{MarAn20}$	20180
K_{LAA}	6473	$\mu_{MarAn20}$	71571
μ_{LAA}	88949	K_{MazE}	57466
K_{RepA70}	5686	μ_{MazE}	32091
μ_{RepA70}	90355	K_{HipB}	48055
K_{SoxS}	19052	μ_{HipB}	43978
μ_{SoxS}	70928	$K_{HipBc20}$	47411
$K_{SoxSn20}$	22340	$\mu_{HipBc20}$	24748
$\mu_{SoxSn20}$	12371		

Supporting Information Captions

Fig. S1. Single degradation tag results with different levels of Dox. An *in vivo* microplate reader assay was used to determine the fluorescence of YFP proteins with and without degradation tags. Symbols (connected by dashed lines) represent the mean fluorescence from four biological replicates, and error bars are the calculated standard deviations from these replicates. Solid lines represent fits to a simple mathematical model (see Methods), with parameters given in Table S3. SoxSn20 tagged proteins deviated noticeably from our model fit, but were included in our fitting analysis. RepA15 tagged proteins were excluded from our model fit due to weak degradation and irregular response, though we still report the corresponding percent degradation in Fig. 2.

Fig. S2. Proteins engineered with the HipB tag and co-produced with (C) RepA70, (D) MarA, and (E) MarAn20 tagged proteins had no detectable crosstalk. YFP derivatives were expressed from the P_{LtetO} promoter using the inducer Dox; while CFP derivatives were expressed from $P_{lac/ara}$ promoter using 0.5 mM IPTG (all experiments contained 1% arabinose). Each tag comparison is indicated by tag/tag with CFP being the first tagged protein and YFP being the second tagged protein. Four biological replicas were used to calculate the mean fluorescence and standard deviation from *in vivo* microplate reader batch data. FU: arbitrary fluorescence unit.

Fig. S3. Analysis of crosstalk using both single-cell and batch data with HipB-tagged proteins. See Fig. 5 and the Method section for details on acquisition and analysis of the single-cell data and microplate batch data.

Fig. S4. Test for bleed-through from one channel to another in *in vivo* microplate reader experiments. No apparent bleed-through was detected in the (**A**) CFP channel when YFP was produced and no apparent bleed-through was detected in the (**B**) YFP channel when CFP was produced. Bleed-through was tested with the *E. coli* strains carrying both untagged fluorescent proteins CFP and YFP. (**C**) No apparent bleed-through was detected in the CFP channel when YFP was produced. (**D**) No apparent bleed-through was detected in the YFP channel when CFP was produced. Dox was used to induce YFP expression and IPTG (with 1% arabinose) was used to induce CFP expression. Four biological replicas were used to calculate the mean fluorescence and standard deviation. FU: arbitrary fluorescence unit.

Fig. S5. Test for bleed-through from one channel to another in single-cell snapshot experiments. No apparent bleed-through was detected in the CFP channel when YFP was produced and no apparent bleed-through was detected in the YFP channel when CFP was produced. Bleed-through was tested with the *E. coli* strains carrying no fluorescent proteins and untagged fluorescent proteins CFP and YFP. When YFP was produced the CFP channel had no apparent change indicated; the CFP channel when YFP had similar mean fluorescence as the CFP channel with no fluorescent proteins (the mean values were within 1 SEM). The same was true when the CFP was produced and the YFP channel was monitored. Dox 200 ng/ml was used to induce YFP expression and 0.5 mM IPTG + 1% arabinose was used to induce CFP expression. Four biological replicas were used to calculate the mean fluorescence and standard deviation. FU: arbitrary fluorescence unit. Single-cell data was acquired by imaging cells at 1000X magnification using a fluorescent confocal microscope with an exposure of 75 ms and light intensity of 6% for both the CFP and YFP channel. Cells were identified and fluorescence levels were calculated using Fiji, machine learning, and in-house scripts (see Methods). The mean and SEM were calculated from 10-19 individual cells.

Fig. S6. Method for Single Cell Analysis. (**a**) To extract single cell fluorescence data, phase contrast images (shown) were taken in sequence with fluorescence images. Phase contrast images generally contained both cells in focus and out of focus. (**b**) Machine learning-based classification (see Methods) was applied to phase contrast images to identify individual cells that were in focus (cells indicated by colored regions). The regions in the image associated with individual cells were then used to measure fluorescence in corresponding images.

References

1. Scott, M.; Klumpp, S.; Mateescu, E. M.; Hwa, T., Emergence of robust growth laws from optimal regulation of ribosome synthesis. *Molecular systems biology* **2014,** *10* (8).
2. Weisse, A. Y.; Oyarzun, D. A.; Danos, V.; Swain, P. S., Mechanistic links between cellular trade-offs, gene expression, and growth. *Proceedings of the National Academy of Sciences of the United States of America* **2015,** *112* (9), E1038-47.
3. Rowland, M. A.; Fontana, W.; Deeds, E. J., Crosstalk and Competition in Signaling Networks. *Biophys J* **2012,** *103* (11), 2389-2398.
4. Rowland, M. A.; Deeds, E. J., Crosstalk and the evolution of specificity in two-component signaling (vol 111, pg 5550, 2014). *Proceedings of the National Academy of Sciences of the United States of America* **2014,** *111* (25), 9325-9325.
5. Flynn, J. M.; Neher, S. B.; Kim, Y. I.; Sauer, R. T.; Baker, T. A., Proteomic discovery of cellular substrates of the ClpXP protease reveals five classes of ClpX-recognition signals. *Molecular cell* **2003,** *11* (3), 671-83.
6. Schweder, T.; Lee, K. H.; Lomovskaya, O.; Matin, A., Regulation of Escherichia coli starvation sigma factor (sigma s) by ClpXP protease. *Journal of bacteriology* **1996,** *178* (2), 470-6.
7. Zhou, Y.; Gottesman, S., Regulation of proteolysis of the stationary-phase sigma factor RpoS. *Journal of bacteriology* **1998,** *180* (5), 1154-8.
8. Cookson, N. A.; Mather, W. H.; Danino, T.; Mondragon-Palomino, O.; Williams, R. J.; Tsimring, L. S.; Hasty, J., Queueing up for enzymatic processing: correlated signaling through coupled degradation. *Molecular systems biology* **2011,** *7*, 561.
9. Himeno, H.; Kurita, D.; Muto, A., tmRNA-mediated trans-translation as the major ribosome rescue system in a bacterial cell. *Frontiers in genetics* **2014,** *5*, 66.
10. Janssen, B. D.; Hayes, C. S., THE tmRNA RIBOSOME-RESCUE SYSTEM. *Adv Protein Chem Str* **2012,** *86*, 151-191.
11. Cameron, D. E.; Bashor, C. J.; Collins, J. J., A brief history of synthetic biology. *Nat Rev Microbiol* **2014,** *12* (5), 381-390.
12. Stricker, J.; Cookson, S.; Bennett, M. R.; Mather, W. H.; Tsimring, L. S.; Hasty, J., A fast, robust and tunable synthetic gene oscillator. *Nature* **2008,** *456* (7221), 516-9.
13. Mather, W.; Bennett, M. R.; Hasty, J.; Tsimring, L. S., Delay-Induced Degrade-and-Fire Oscillations in Small Genetic Circuits. *Phys Rev Lett* **2009,** *102* (6).
14. Mather, W. H.; Cookson, N. A.; Hasty, J.; Tsimring, L. S.; Williams, R. J., Correlation Resonance Generated by Coupled Enzymatic Processing. *Biophys J* **2010,** *99* (10), 3172-3181.
15. Hochendoner, P.; Ogle, C.; Mather, W. H., A queueing approach to multi-site enzyme kinetics. *Interface focus* **2014,** *4* (3), 20130077.
16. Butzin, N. C.; Hochendoner, P.; Ogle, C. T.; Mather, W. H., Entrainment of a Bacterial Synthetic Gene Oscillator through Proteolytic Queueing. *ACS synthetic biology* **2016**.
17. Rondelez, Y., Competition for Catalytic Resources Alters Biological Network Dynamics. *Phys Rev Lett* **2012,** *108* (1).
18. Butzin, N. C.; Mather, W. H., Synthetic Genetic Oscillators. In *Reviews in Cell Biology and Molecular Medicine*, Wiley-VCH Verlag GmbH & Co. KGaA: 2016.
19. Potvin-Trottier, L.; Lord, N. D.; Vinnicombe, G.; Paulsson, J., Synchronous long-term oscillations in a synthetic gene circuit. *Nature* **2016,** *538* (7626), 514-517.
20. Ogle, C. T.; Mather, W. H., Proteolytic crosstalk in multi-protease networks. *Physical Biology* **2016,** *13* (2).
21. Maurizi, M. R., Proteases and protein degradation in Escherichia coli. *Experientia* **1992,** *48* (2), 178-201.

22. Kuroda, A.; Nomura, K.; Ohtomo, R.; Kato, J.; Ikeda, T.; Takiguchi, N.; Ohtake, H.; Kornberg, A., Role of inorganic polyphosphate in promoting ribosomal protein degradation by the Lon protease in E. coli. *Science* **2001,** *293* (5530), 705-8.
23. Wickner, S.; Maurizi, M. R.; Gottesman, S., Posttranslational quality control: folding, refolding, and degrading proteins. *Science* **1999,** *286* (5446), 1888-93.
24. Gottesman, S.; Roche, E.; Zhou, Y.; Sauer, R. T., The ClpXP and ClpAP proteases degrade proteins with carboxy-terminal peptide tails added by the SsrA-tagging system. *Genes & development* **1998,** *12* (9), 1338-47.
25. Brehm-Stecher, B. F.; Johnson, E. A., Single-cell microbiology: tools, technologies, and applications. *Microbiol Mol Biol Rev* **2004,** *68* (3), 538-59, table of contents.
26. Butzin, N. C.; Hochendoner, P.; Ogle, C. T.; Hill, P.; Mather, W. H., Marching along to an Offbeat Drum: Entrainment of Synthetic Gene Oscillators by a Noisy Stimulus. *ACS synthetic biology* **2015**.
27. Elowitz, M. B.; Leibler, S., A synthetic oscillatory network of transcriptional regulators. *Nature* **2000,** *403* (6767), 335-8.
28. Fung, E.; Wong, W. W.; Suen, J. K.; Bulter, T.; Lee, S. G.; Liao, J. C., A synthetic gene-metabolic oscillator. *Nature* **2005,** *435* (7038), 118-22.
29. Wong, W. W.; Tsai, T. Y.; Liao, J. C., Single-cell zeroth-order protein degradation enhances the robustness of synthetic oscillator. *Molecular systems biology* **2007,** *3*, 130.
30. Prindle, A.; Selimkhanov, J.; Danino, T.; Samayoa, P.; Goldberg, A.; Bhatia, S. N.; Hasty, J., Genetic Circuits in Salmonella typhimurium. *ACS synthetic biology* **2012,** *1* (10), 458-464.
31. Mondragon-Palomino, O.; Danino, T.; Selimkhanov, J.; Tsimring, L.; Hasty, J., Entrainment of a population of synthetic genetic oscillators. *Science* **2011,** *333* (6047), 1315-9.
32. Hussain, F.; Gupta, C.; Hirning, A. J.; Ott, W.; Matthews, K. S.; Josic, K.; Bennett, M. R., Engineered temperature compensation in a synthetic genetic clock. *Proceedings of the National Academy of Sciences of the United States of America* **2014,** *111* (3), 972-7.
33. Danino, T.; Mondragon-Palomino, O.; Tsimring, L.; Hasty, J., A synchronized quorum of genetic clocks. *Nature* **2010,** *463* (7279), 326-30.
34. Prindle, A.; Samayoa, P.; Razinkov, I.; Danino, T.; Tsimring, L. S.; Hasty, J., A sensing array of radically coupled genetic 'biopixels'. *Nature* **2012,** *481* (7379), 39-44.
35. Prindle, A.; Selimkhanov, J.; Li, H.; Razinkov, I.; Tsimring, L. S.; Hasty, J., Rapid and tunable post-translational coupling of genetic circuits. *Nature* **2014,** *508* (7496), 387-91.
36. Schindelin, J.; Arganda-Carreras, I.; Frise, E.; Kaynig, V.; Longair, M.; Pietzsch, T.; Preibisch, S.; Rueden, C.; Saalfeld, S.; Schmid, B.; Tinevez, J. Y.; White, D. J.; Hartenstein, V.; Eliceiri, K.; Tomancak, P.; Cardona, A., Fiji: an open-source platform for biological-image analysis. *Nature methods* **2012,** *9* (7), 676-82.
37. Wickner, S.; Gottesman, S.; Skowyra, D.; Hoskins, J.; McKenney, K.; Maurizi, M. R., A molecular chaperone, ClpA, functions like DnaK and DnaJ. *Proceedings of the National Academy of Sciences of the United States of America* **1994,** *91* (25), 12218-22.
38. Hoskins, J. R.; Kim, S. Y.; Wickner, S., Substrate recognition by the ClpA chaperone component of ClpAP protease. *The Journal of biological chemistry* **2000,** *275* (45), 35361-7.
39. Hoskins, J. R.; Singh, S. K.; Maurizi, M. R.; Wickner, S., Protein binding and unfolding by the chaperone ClpA and degradation by the protease ClpAP. *Proceedings of the National Academy of Sciences of the United States of America* **2000,** *97* (16), 8892-7.
40. Hoskins, J. R.; Yanagihara, K.; Mizuuchi, K.; Wickner, S., ClpAP and ClpXP degrade proteins with tags located in the interior of the primary sequence. *Proceedings of the National Academy of Sciences of the United States of America* **2002,** *99* (17), 11037-42.
41. Hoskins, J. R.; Wickner, S., Two peptide sequences can function cooperatively to facilitate binding and unfolding by ClpA and degradation by ClpAP. *Proceedings of the National Academy of Sciences of the United States of America* **2006,** *103* (4), 909-14.

42. Griffith, K. L.; Shah, I. M.; Wolf, R. E., Jr., Proteolytic degradation of Escherichia coli transcription activators SoxS and MarA as the mechanism for reversing the induction of the superoxide (SoxRS) and multiple antibiotic resistance (Mar) regulons. *Molecular microbiology* **2004,** *51* (6), 1801-16.
43. Tsilibaris, V.; Maenhaut-Michel, G.; Van Melderen, L., Biological roles of the Lon ATP-dependent protease. *Research in microbiology* **2006,** *157* (8), 701-13.
44. Gerdes, K.; Maisonneuve, E., Bacterial persistence and toxin-antitoxin loci. *Annual review of microbiology* **2012,** *66*, 103-23.
45. Hansen, S.; Vulic, M.; Min, J.; Yen, T. J.; Schumacher, M. A.; Brennan, R. G.; Lewis, K., Regulation of the Escherichia coli HipBA toxin-antitoxin system by proteolysis. *PloS one* **2012,** *7* (6), e39185.
46. Schumacher, M. A.; Piro, K. M.; Xu, W.; Hansen, S.; Lewis, K.; Brennan, R. G., Molecular mechanisms of HipA-mediated multidrug tolerance and its neutralization by HipB. *Science* **2009,** *323* (5912), 396-401.
47. Volkert, M. R.; Landini, P., Transcriptional responses to DNA damage. *Curr Opin Microbiol* **2001,** *4* (2), 178-85.
48. Alekshun, M. N.; Levy, S. B., The mar regulon: multiple resistance to antibiotics and other toxic chemicals. *Trends Microbiol* **1999,** *7* (10), 410-3.
49. Wood, T. K.; Knabel, S. J.; Kwan, B. W., Bacterial persister cell formation and dormancy. *Applied and environmental microbiology* **2013,** *79* (23), 7116-21.
50. Maisonneuve, E.; Gerdes, K., Molecular mechanisms underlying bacterial persisters. *Cell* **2014,** *157* (3), 539-48.
51. del Solar, G.; Giraldo, R.; Ruiz-Echevarria, M. J.; Espinosa, M.; Diaz-Orejas, R., Replication and control of circular bacterial plasmids. *Microbiol Mol Biol Rev* **1998,** *62* (2), 434-64.
52. Gottesman, S., Proteolysis in bacterial regulatory circuits. *Annual review of cell and developmental biology* **2003,** *19*, 565-87.
53. Farrell, C. M.; Grossman, A. D.; Sauer, R. T., Cytoplasmic degradation of ssrA-tagged proteins. *Mol Microbiol* **2005,** *57* (6), 1750-61.
54. Chowdhury, T.; Chien, P.; Ebrahim, S.; Sauer, R. T.; Baker, T. A., Versatile modes of peptide recognition by the ClpX N domain mediate alternative adaptor-binding specificities in different bacterial species. *Protein science : a publication of the Protein Society* **2010,** *19* (2), 242-54.
55. Flynn, J. M.; Levchenko, I.; Seidel, M.; Wickner, S. H.; Sauer, R. T.; Baker, T. A., Overlapping recognition determinants within the ssrA degradation tag allow modulation of proteolysis. *Proceedings of the National Academy of Sciences of the United States of America* **2001,** *98* (19), 10584-9.
56. Dougan, D. A.; Reid, B. G.; Horwich, A. L.; Bukau, B., ClpS, a substrate modulator of the ClpAP machine. *Molecular cell* **2002,** *9* (3), 673-83.

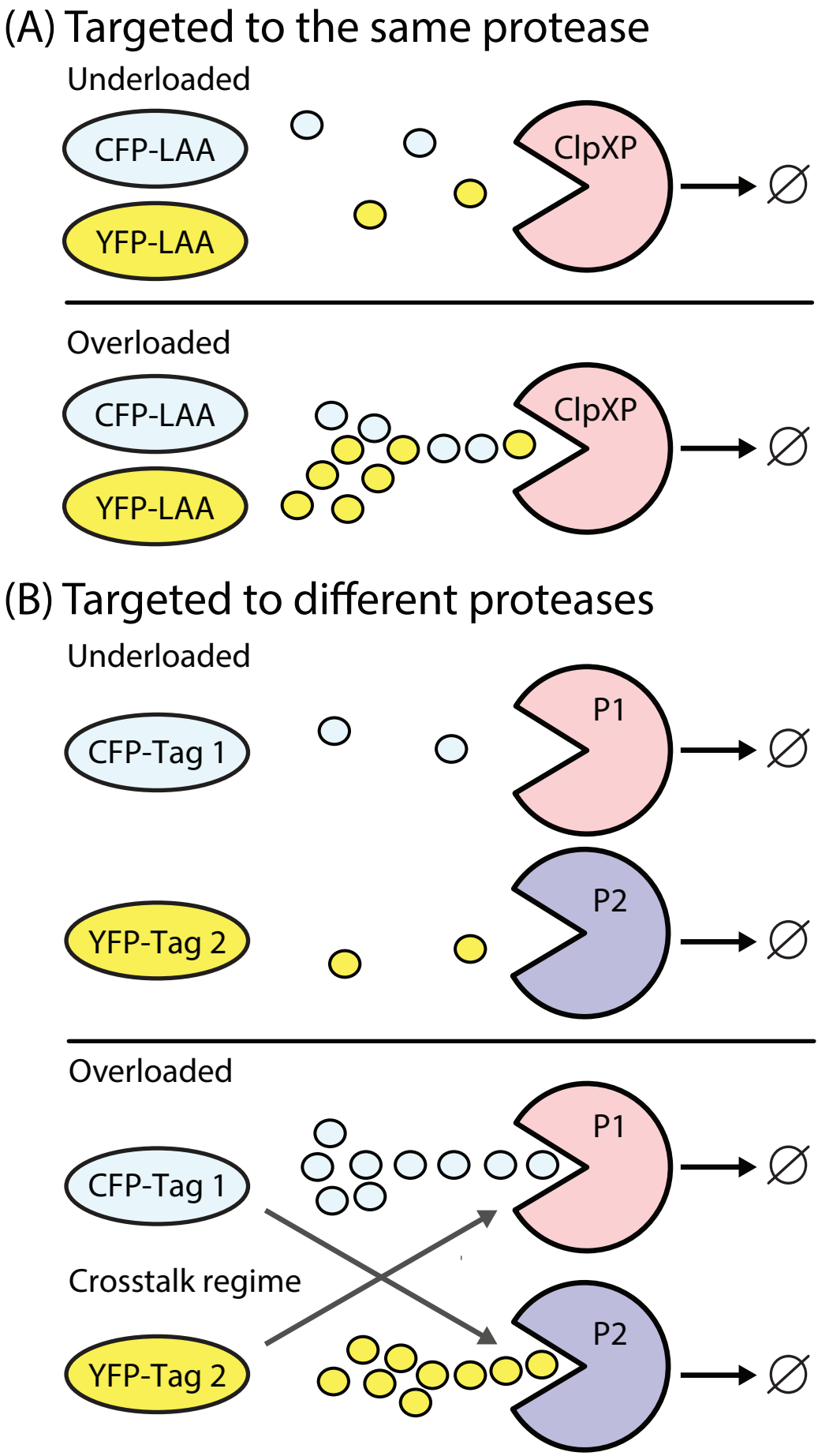
(A) Targeted to the same protease
Underloaded
CFP-LAA
YFP-LAA
ClpXP
∅
Overloaded
CFP-LAA
YFP-LAA
ClpXP
∅
(B) Targeted to different proteases
Underloaded
CFP-Tag 1
YFP-Tag 2
P1
P2
∅
∅
Overloaded
CFP-Tag 1
YFP-Tag 2
Crosstalk regime
P1
P2
∅
∅

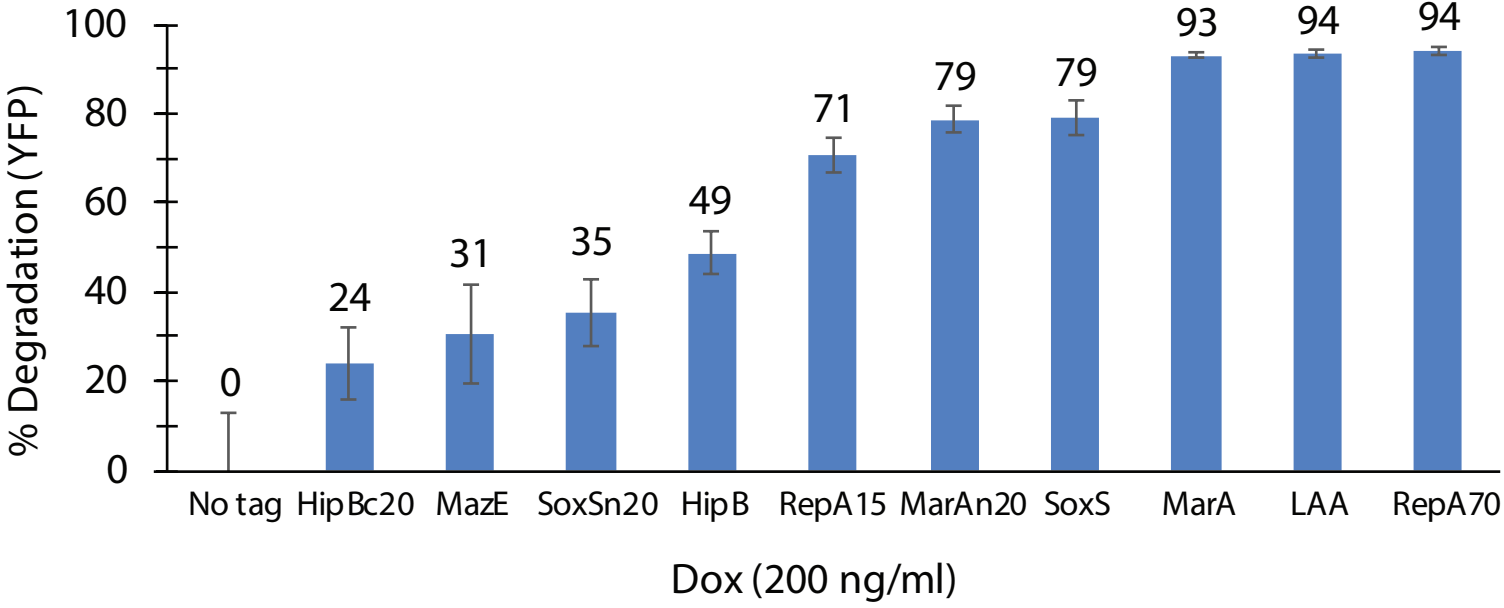
% Degradation (YFP)
100
80
60
40
20
0
0
24
31
35
49
71
79
79
93
94
94
No tag
HipBc20
MazE
SoxSn20
HipB
RepA15
MarAn20
SoxS
MarA
LAA
RepA70
Dox (200 ng/ml)

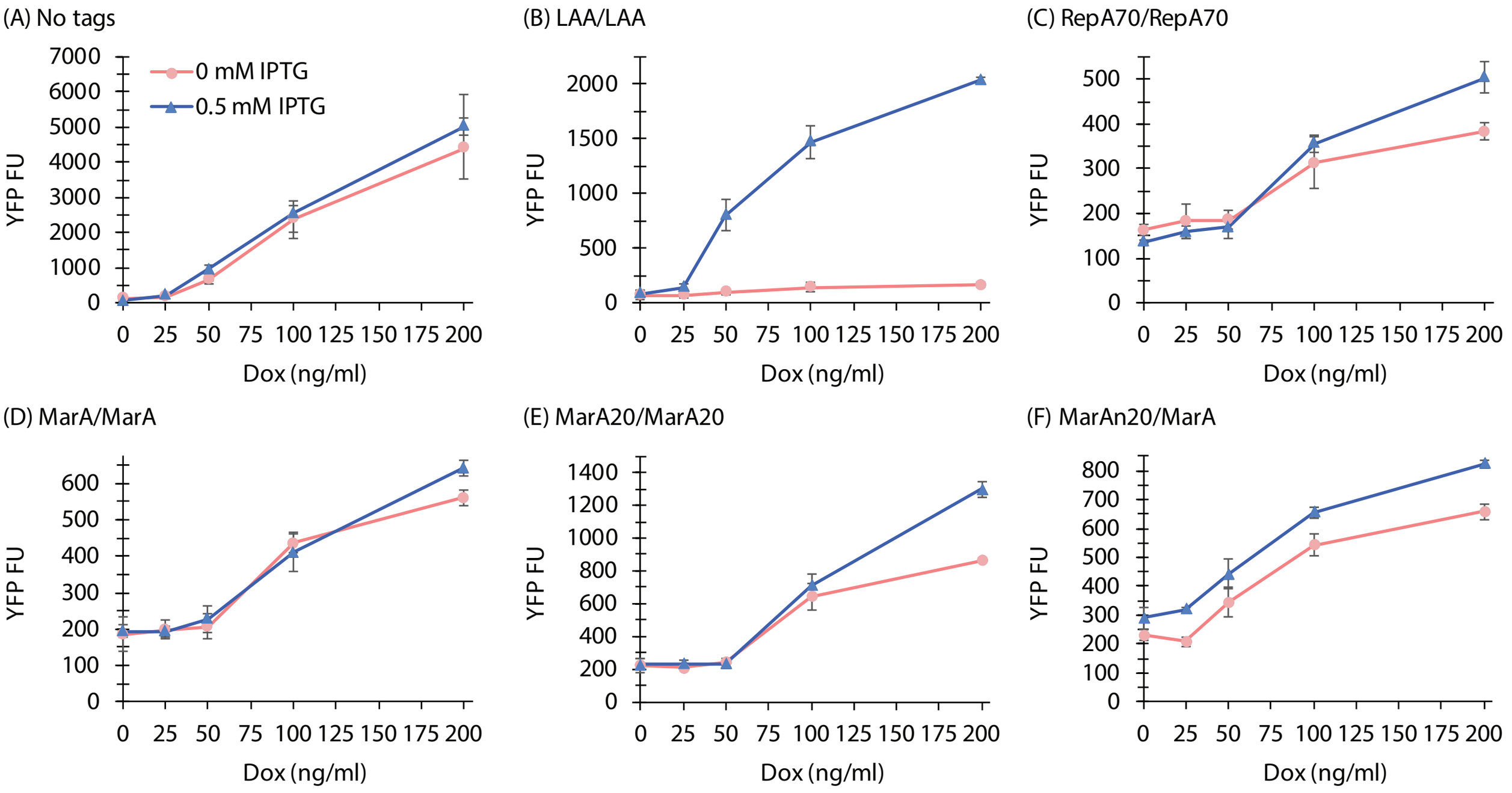
(A) No tags
0 mM IPTG
0.5 mM IPTG
YFP FU
Dox (ng/ml)
(B) LAA/LAA
(C) RepA70/RepA70
(D) MarA/MarA
(E) MarA20/MarA20
(F) MarAn20/MarA

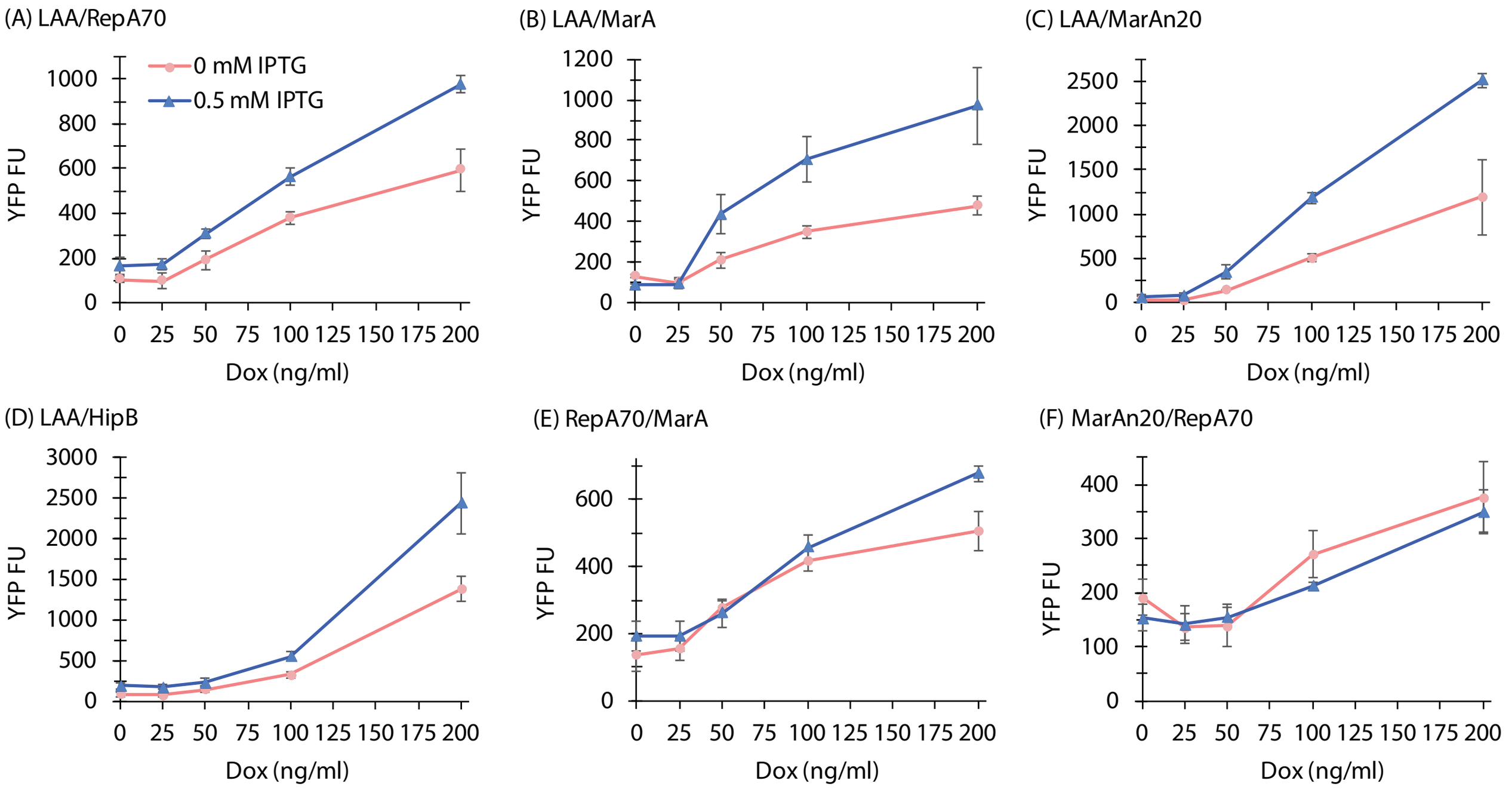
(A) LAA/RepA70
0 mM IPTG
0.5 mM IPTG
YFP FU
Dox (ng/ml)
(B) LAA/MarA
(C) LAA/MarAn20
(D) LAA/HipB
(E) RepA70/MarA
(F) MarAn20/RepA70

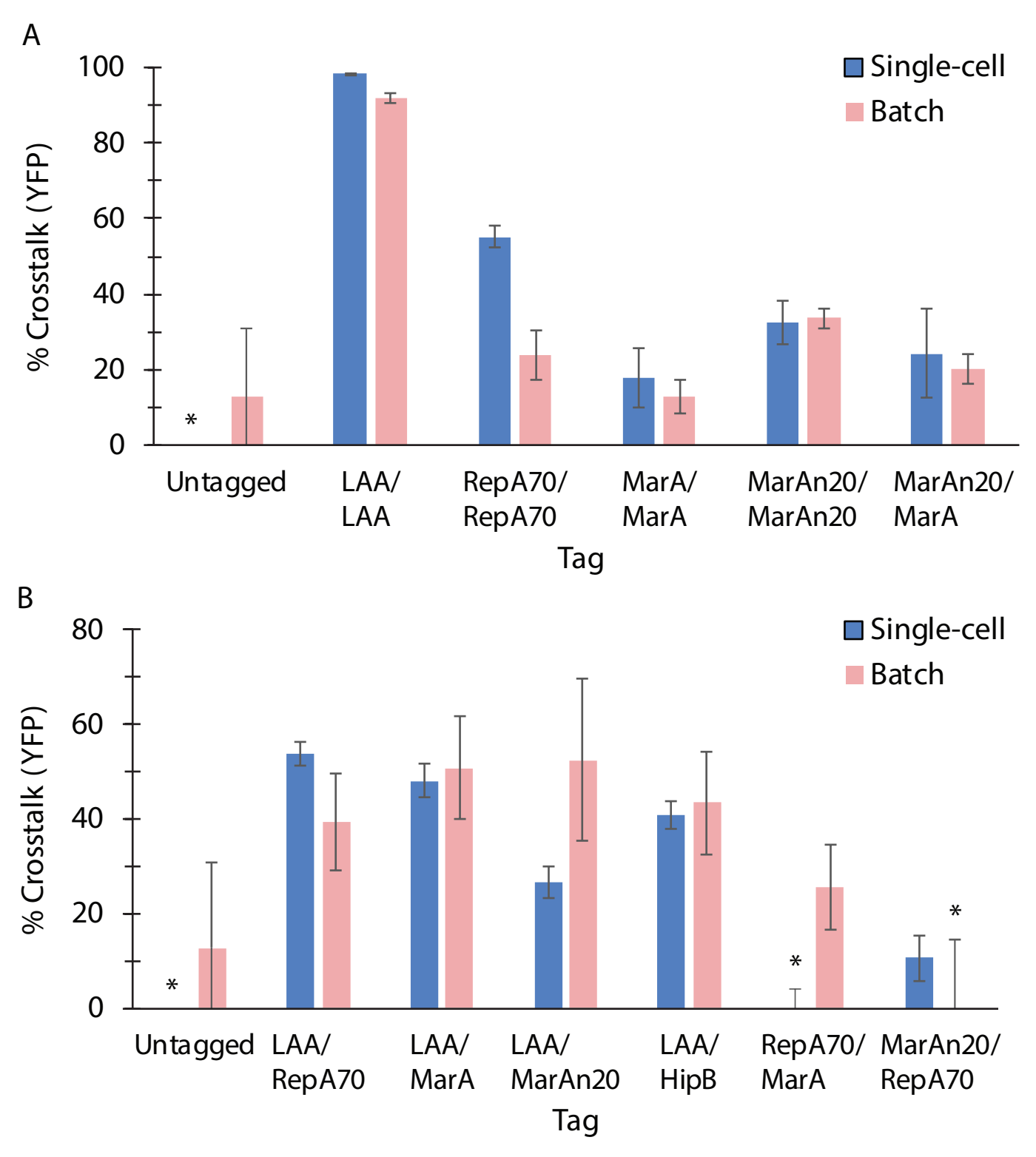
A
100
80
60
40
20
0
% Crosstalk (YFP)
Single-cell
Batch
*
Untagged
LAA/
LAA
RepA70/
RepA70
MarA/
MarA
MarAn20/
MarAn20
MarAn20/
MarA
Tag
B
80
60
40
20
0
% Crosstalk (YFP)
Single-cell
Batch
*
*
*
Untagged
LAA/
RepA70
LAA/
MarA
LAA/
MarAn20
LAA/
HipB
RepA70/
MarA
MarAn20/
RepA70
Tag